A Study on the Torsional Vibration Characteristics of Super Large Two Stroke Low Speed Diesel Engines with Tuning Damper

튜닝댐퍼를 갖는 초대형 저속 2행정 디젤엔진의 비틀림진동 특성에 관한 연구

Don Chool Lee† and Ronald D. Barro*
이 돈 출·로날드 디. 바로

(Received October 16, 2008 ; Accepted December 23, 2008)

Key Words : Torsional Vibration(비틀림진동), Tuning Damper(튜닝댐퍼), Two Stroke Low Speed Diesel Engine(저속 2행정 디젤엔진)

ABSTRACT

The shipbuilder's requirement for a higher power output rating has led to the development of a super large two stroke low speed diesel engines. Usually a large-sized bore engine ranging from 8~14 cylinders, this engine group is capable of delivering power output of more than 100,000 bhp at maximum continuous rating(mcr). Other positive aspects of this engine type include higher thermal efficiency, reliability, durability and mobility. This plays a vital role in meeting the propulsion requirement of vessels, specifically for large container ships, of which speed is a primary concern to become more competitive. Consequently, this also resulted in the modification of engine parameters and new component designs to meet the consequential higher mean effective pressure and higher maximum combustion pressure. Even though the fundamental excitation mechanisms unchanged, torsional vibration stresses in the propulsion shafting are subsequently perceived to be higher. As such, one important viewpoint in the initial engine design is the resulting vibration characteristic expected to prevail on the propulsion shafting system(PSS). This paper investigated the torsional vibration characteristics of these super large engines. For the two node torsional vibration with a nodal point on the crankshaft, a tuning damper is necessary to reduce the torsional stresses on the crankshaft. Hence, the tuning torsional vibration damper design and compatibility to the shafting system was similarly reviewed and analyzed.

요 약

최근 조선소에서 고출력 디젤엔진의 요구에 의해서 초대형 저속 2행정 디젤엔진이 개발되었으며, 연속최대출력이 8~14실린더를 갖는 10만 마력 이상의 엔진을 사용할 수 있게 되었다. 이러한 엔진들은 열효율, 운전에 대한 신뢰성, 강인성 및 기동성은 뛰어나지만 크랭크축을 포함한 추진축계에서 높은 비틀림진동을 유발한다. 따라서 이 연구에서는 엔진설계자의 입장에서 비틀림진동을 줄이기 위하여 튜닝 비틀림진동 댐퍼를 갖

† Corresponding Author ; Member, Mokpo National Maritime University
Tel : (061)240-7219, Fax : (061) 240-7201
E-mail : ldcvib@mmu.ac.kr
* Philippine Merchant Marine Academy

는 추진축계의 비틀림진동을 이론적으로 검토하였으며 실험모델인 12K98MC엔진과 12RT-flex엔진에서 튜닝댐퍼의 성능과 동적거동을 확인하고 있다.

Nomenclatures

α : Explosion phase angle of the i^{th} cylinder
β_i : The i^{th} torsional angle
$\Delta\beta_i$: $\beta_i - \beta_{i+1}$
$c_c(=2I_d\omega_0)$: Critical damping coefficient
$\gamma(=c/c_c)$: Ratio of damping coefficients
I_i : The i^{th} moment of inertia
i : Number of lumped masses
k_i : Torsional stiffness of the i^{th} lumped mass
m : Total number of cylinders
n : Total number of lumped masses
$\nu(=\omega_d/\omega_0)$: Ratio of damper natural angular frequency to PSS
$\lambda(=\omega/\omega_0)$: Ratio of excitation frequency to natural angular frequency of PSS
ω : Angular velocity
$\omega_0^2(=k/I)$: Natural angular frequency of the PSS
$\omega_d^2(=k_d/I_d)$: Natural angular frequency of the damper
$R(=I_d/I)$: Ratio of inertia moments
T_{io} : Excitation torque to each cylinder
$\theta_{st}(=T_0/k)$: Static angle displacement of the PSS

1. Introduction

Two stroke low speed diesel engine has shown significant developments since its initial conception. From then, increased mean effective pressures and higher thermal efficiency has been the designer's continued priorities. Some recent advancement affirmed the efforts with the introduction of engines capable of delivering power output above the 100,000 bhp mark[1]. These developments, however, also resulted in increased exciting torques and stresses resulting to several complicated vibration problems.

One of these vibration phenomena is the torsional vibration which demands a thorough understanding of its effect on the system. This vibration affects all rotating machinery and must be investigated thoroughly as it has a significant influence on the engine, hull and shafting system. Torsional analysis of the propulsion shafting system should be given considerations in the early design stage, thereby identifying the significant resonance conditions[2]. Torsional vibration is defined as the inertia or rigid body oscillations about the central axis of the shaft line, or simply as the twist and its resonance caused by the explosion(gas) pressure and the inertia forces of cylinder and piston in reciprocating internal combustion engines[3].

For the large-sized bore of 8~12, and 14 cylinders, the torsional vibration stresses and vibratory torque at the two node torsional vibration with a nodal point located at the crankshaft was emphasized[4,5]. Two twelve (12) cylinder engines with a 980 mm and 960 mm bore were employed as case study models. This study investigated the dynamic characteristics of torsional vibrations of super large two stroke low speed engines with tuning damper. Onboard measurements were carried out to confirm the theoretical calculated value of the torsional vibration stresses of the PSS. Likewise, the angular velocities of the turning(fly) wheel were measured and the function of the Geislinger tuning damper was confirmed through its monitoring system.

2. Tuning Damper Basic Theory for Optimum Design[6,7]

The ship's propulsion shafting and damping system is actually regarded as a multi-degree of

freedom system. However, it can be replaced by an equivalent inertia and stiffness forced vibration system, as can be seen in Fig. 1, for calculation simplicity. For the case of damper design, an equivalent inertia moment I of the corresponding systems is $\sum_{i=1}^{n} I_i \beta_i^2$ and the equivalent stiffness k is $\sum_{i=1}^{n} k_i \left(\Delta \beta_i^2\right)$. The resultant vector of engine cylinder's excitation torque is $\sum_{i=1}^{m} \beta_i T_{io} \cos\left(\omega t + \alpha\right)$, but for a two lumped mass system application when the phase lag is neglected it becomes $T_o \cos \omega t$.

A resonance will occur in the damper if the natural angular frequency of main vibration system $\omega_o\left(\sqrt{k/I}\right)$ is equal to the damper $\omega_d\left(\sqrt{k_d/I_d}\right)$. It can be noted that for a system under free vibration conditions, that is without a exciting torque T=0, $\sum J\omega^2\theta = 0$ will be attained if ω is the natural frequency[8].

When the damping coefficient of dash-pot c and the damper stiffness k_d and inertia mass moment I_d are attached to the main vibration system, and the corresponding angle amplitude are θ_1 and θ_2 respectively, then kinetic energy(T), elastic energy(U) and viscous energy(F) can be presented in the following equation:

$$2T = I\dot{\theta}_1^2 + I_d\dot{\theta}_2^2 \tag{1}$$

$$2U = k\theta_1^2 + k_d\left(\theta_2 - \theta_1\right)^2 \tag{2}$$

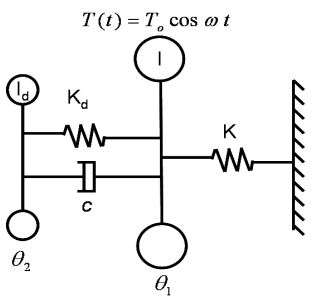

Fig. 1 Two mass-torsional spring system model for torsional tuning damper

$$2F = c\left(\dot{\theta}_2 - \dot{\theta}_1\right)^2 \tag{3}$$

When excitation torque $T_o \cos \omega t$ is applied to an equivalent inertia moment I, the equations of motion of the two masses can be given as

$$I\ddot{\theta}_1 + k\theta_1 - k_d\left(\theta_2 - \theta_1\right) - c\left(\dot{\theta}_2 - \dot{\theta}_1\right) = T_o \cos \omega t \tag{4}$$

$$I_d\ddot{\theta}_2 + k_d\left(\theta_2 - \theta_1\right) + c\left(\dot{\theta}_2 - \dot{\theta}_1\right) = 0 \tag{5}$$

In order to solve the forced vibration problems, only the real part of the solution is considered and $\dot{\theta}_1, \ddot{\theta}_1, \dot{\theta}_2$, and $\ddot{\theta}_2$ will be obtained. The steady state solution of Eqs. (4) and (5) will be obtained as

$$\theta_1 = \mathrm{Re}\left[\frac{T_0 e^{i\omega t}\left[\left(k_d - I_d\omega^2\right) + i\omega c\right]}{\left[\left(k - I\omega^2\right)\left(k_d - I_d\omega^2\right) - I_d k_d\omega^2\right] + i\omega c\left(k - I\omega^2 - I_d\omega^2\right)}\right] \tag{6}$$

$$\theta_2 = \mathrm{Re}\left[\frac{T_0 e^{i\omega t}\left(k_d + i\omega c\right)}{\left[\left(k - I\omega^2\right)\left(k_d - I_d\omega^2\right) - I_d k_d\omega^2\right] + i\omega c\left(k - I\omega^2 - I_d\omega^2\right)}\right] \tag{7}$$

The absolute values of θ_1 and $\tan\delta_1$ in Equations (6) and (7) becomes

$$\theta_2 - \theta_1 = \mathrm{Re}\left[\frac{T_0 e^{i\omega t} I_d\omega^2}{\left[\left(k - I\omega^2\right)\left(k_d - I_d\omega^2\right) - I_d k_d\omega^2\right] + i\omega c\left(k - I\omega^2 - I_d\omega^2\right)}\right] \tag{8}$$

$$\theta_1 = \left[\frac{\left(k_d - I_d\omega^2\right)^2 + \left(\omega c\right)^2}{\left[\left(k - I\omega^2\right)\left(k_d - I_d\omega^2\right) - I_d k_d\omega^2\right]^2 + \left(\omega c\right)^2\left(k - I\omega^2 - I_d\omega^2\right)^2}\right] \times T_0 \cos\left(\omega t - \delta_1\right) \tag{9}$$

$$\tan\delta_1 = \left[\frac{\omega c\left(I_d\omega^2\right)^2}{\left[\left(k - I\omega^2\right)\left(k_d - I_d\omega^2\right) - I_d k_d\omega^2\right]\left(k_d - I_d\omega^2\right) + \left(\omega c\right)^2\left(k - I\omega^2 - I_d\omega^2\right)}\right] \tag{10}$$

Eqs. (6)~(10) can be rearranged to Eqs. (11) to (16). Hence, the magnitudes, A_1 and A_2, can be expressed as

$$\theta_1/\theta_{st} = A_1\cos(\omega t - \delta_1)$$

$$A_1 = \left[\frac{(v^2-\lambda^2)^2 + (2\gamma\lambda)^2}{(2\gamma\lambda)^2\{1-(1+R)\lambda^2\}^2 + \{(1-\lambda^2)(v^2-\lambda^2) - Rv^2\lambda^2\}^2}\right]^{1/2} \tag{11}$$

$$\delta_1 = \left[\frac{2\gamma\lambda(R\lambda^4)}{\{(1-\lambda^2)(v^2-\lambda^2) - Rv^2\lambda^2\}(v^2-\lambda^2) + (2\gamma\lambda)^2\{1-(1+R)\lambda^2\}}\right] \tag{12}$$

$$\theta_2/\theta_{st} = A_2\cos(\omega t - \delta_2)$$

$$A_2 = \left[\frac{v^4 + (2\gamma\lambda)^2}{(2\gamma\lambda)^2\{1-(1+R)\lambda^2\}^2 + \{(1-\lambda^2)(v^2-\lambda^2) - Rv^2\lambda^2\}^2}\right]^{1/2} \tag{13}$$

$$\delta_2 = \tan^{-1}\left[\frac{(2\gamma\lambda)\lambda^2(1-\lambda^2)}{v^2\{(1-\lambda^2)(v^2-\lambda^2) - Rv^2\lambda^2\} + (2\gamma\lambda)^2\{1-(1+R)\lambda^2\}}\right] \tag{14}$$

Tuning dampers are usually employed for the purpose of enhancing the damping effect by enlarging the relative motion, that is, θ_{12} which is induced by resonance between damper and the main shafting systems. Hence,

$$(\theta_2 - \theta_1)/\theta_{st} = A_{12}\cos(\omega t - \delta_{12})$$

$$A_{12} = \frac{\lambda^2}{\left[(2\gamma\lambda)^2\{1-(1+R)\lambda^2\}^2 + \{(1-\lambda^2)(v^2-\lambda^2) - Rv^2\lambda^2\}^2\right]^{1/2}} \tag{15}$$

$$\delta_{12} = \tan^{-1}\left[\frac{(2\gamma\lambda)\{1-(1+R)\lambda^2\}}{(1-\lambda^2)(v^2-\gamma^2) - Rv^2\lambda^2}\right]^{1/2} \tag{16}$$

Equation (11) shows that the amplitude of vibration of the main system $\lambda = \omega/\omega_o$ is a function of R, v, λ and γ.

Figure 2 shows the graph of the variation in magnification factor A_1 for different damper damping coefficients and, where R=1/20 and the ratio of the natural frequency v=1 are taken.

It will be noted that even if different damping coefficients of damper are given, the response curves will pass through a common point P and Q. The points P and Q can be located by substituting the extreme values of γ=0 and $\gamma = \infty$ into Eq. (11) to give :

$$(A_1)_{\gamma=0} = \frac{v^2-\lambda^2}{(1-\lambda^2)(v^2-\lambda^2) - Rv^2\lambda^2} \tag{17}$$

$$(A_1)_{\gamma=\infty} = \frac{1}{1-(1+R)\lambda^2} \tag{18}$$

The optimum design criterion requires that the heights of P and Q be equal so that $(A_1)_{\gamma=0}(P) = -(A_1)_{\gamma=\infty}(Q)$. The negative sign on the Q point indicates the 180 degrees phase difference between P and Q points around the resonance condition. Hence, the resulting equation gives:

$$(2+R)\lambda^4 - 2\lambda^2(1+v^2+Rv^2) + 2v^2 = 0 \tag{19}$$

In addition, A_1 at P and Q points for $\gamma = \infty$ corresponds to Eq. (18) from which Eq. (20) can be obtained and is rearranged to give Eq. (21).

$$\frac{1}{1-(1+R)\lambda_P^2} = -\frac{1}{1-(1+R)\lambda_Q^2} \tag{20}$$

$$\lambda_P^2 + \lambda_Q^2 = \frac{2}{1+R} \tag{21}$$

$\lambda_P^2 + \lambda_Q^2$ in Eq. (21) is equivalent to the sum

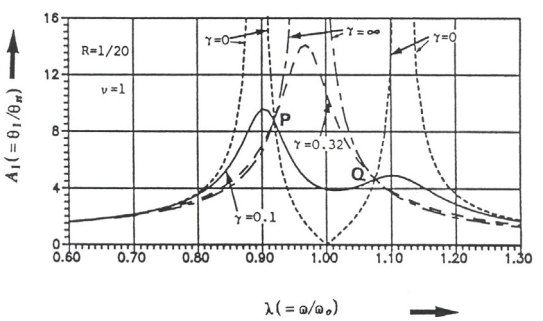

Fig. 2 Effect of vibration damper on the vibratory system response

of two solutions of Eq. (19) for λ^2 and Eq. (22) can be derived.

$$\frac{2}{1+R} = \frac{2\left(1+v^2+Rv^2\right)}{2+R} \tag{22}$$

Therefore, the condition of natural frequency ratio being equal at the same height of P and Q points corresponds to Eq. (23). A damper which satisfies this condition can then be termed as a tuned vibration damper[9].

$$v = \frac{1}{1+R} \tag{23}$$

However, Eq. (23) does not indicate the optimal value of damping ratio γ and the corresponding value of A_1. As such, Eq. (23) can be substituted into Eq. (11). The condition of amplitudes of P and Q points being maximum values can be then calculated as follows:

$$\begin{aligned} &\partial A_1/\partial\lambda = 0 \\ &\gamma_P^2 = \frac{R}{8(1+R)^3}\left(3-\sqrt{\frac{R}{2+R}}\right), \\ &\gamma_Q^2 = \frac{R}{8(1+R)^3}\left(3+\sqrt{\frac{R}{2+R}}\right) \end{aligned} \tag{24}$$

Referring to Eq. (23), the optimum ratio of the damping coefficients at P and Q points takes different values but taking the average values will not cause much difference in the A_1 values. Hence the convenient optimal value of γ^2 can be given by Eq. (25).

$$\gamma_{optimal}^2 = \frac{3R}{8(1+R)^3} \tag{25}$$

For the optimal value of A_1 , λ_P and λ_Q can be reduced using Eqs. (19) and (23) to give Eq. (26). Thereby, A_1 becomes Eq. (27).

$$\lambda_P^2, \lambda_Q^2 = \frac{1}{1+R} \pm \frac{1}{1+R}\sqrt{\frac{R}{2+R}} \tag{26}$$

$$\left|A_1\right|_{optimal} = \sqrt{1+\frac{2}{R}} \tag{27}$$

Furthermore, the principle of an actual ship design requires that the angular natural frequency of damper $\omega_d\left(\sqrt{K_d/I_d}\right)$ be slightly lower than ω_0 which corresponds to the natural frequency of main engine before dampers are installed. In this case, resonance will occur between inner and outer rings of the entire system and the relative angular velocity increases, thus the damping effect can be increased as well. Besides the optimum design criterion for dampers described previously, some other aspects of damper design also needs to be considered. This includes durability for which the damper spring member should be able to withstand the range of allowable vibration torque. Secondly, since the suggested allowable torsional vibration curves/values differs in each classification society, an economical design can be considered to suit its requirement. Lastly, the appropriate adjustment of P and Q points should also be paid with attention. Two adjusting methods can be done – i.e. adjusting the P point lower the Q point higher than the maximum continuous revolution while the other method is adjusting both P and Q points to be lower than the maximum continuous revolution. For the case of two node torsional vibration with one nodal point located on the crankshaft, it is recommended to locate the P and Q points at the same height following the torsional vibration allowable curve of the classification society.

3. Torsional Vibration Analysis and Measurement of Super Large Two Stroke Low Speed Diesel Engines

For the two node torsional vibration with nodal point located in the crankshaft, a damper is implemented in order to reduce the torsional

vibration stresses. Similarly, a damper is necessary if resonance occurs around the maximum continuous revolution and a barred operation zone (critical speed) can not be assigned. For the purpose of this study, a 12K98MC and a 12RT-flex 96C-B engine were used as case models. Likewise, with the damping coefficient becoming larger in the second node vibration than the one node vibration system, a Geislinger type damper was installed to control the second node vibration.

In a multi-lumped mass system, the propeller, engine and damper will show complex dynamic behaviours. On the other hand, in the actual design process, damper size, stiffness, and optimum damping coefficient are evaluated. The damper and shafting torsional vibration torque can then be calculated and kept within the manufacturer's acceptable levels.

For the two node vibration, the excitation order to be considered is higher than that of a one node vibration. Thus the excitation force(harmonic coefficient) inducing the actual torsional vibration is smaller and the nodal point will be located on the crankshaft. Equally, the equivalent mass of the engine is smaller when compared to the one node vibration system, as well as the torsional angle of the propeller. Therefore, the effect of the equivalent mass of the propeller on the equivalent mass of the propulsion shaft is negligible. Lastly, the phase vector of the excitation force is not equal and for this reason, vibration can be controlled by a relatively small damper compared to the engine size.

Torsional vibration stresses and angular velocities were measured at the intermediate shaft and turning wheel to confirm the torsional stresses of the PSS and the function of the Geislinger tuning damper. The torsional vibration stress measurement was acquired on both the normal firing condition and one cylinder misfiring condition of the engine. A tele-metering system was installed at

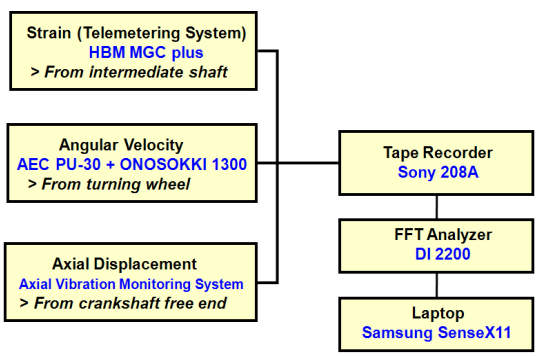

Fig. 3 Schematic diagram for torsional vibration measurement

Table 1 Specification for 12K98MC-Mk6

Engine	Type	12K98MC Mk6
	Max. Continuous output	93,360 bhp
	Max. Continuous speed	94.0 rpm
	Cylinder bore	980.0 mm
	Stroke	2,660.0 mm
	Number of cylinder	12
	Mean indicated pressure	19.5 bar
	Ratio of connecting rod	0.413
	Reciprocating mass	18,149 kg/cyl
	Firing order	1-8-12-4-2-9-10-5-3-7-11-6
Damper	Type	Geislinger D280/11
	Inner inertia	1,410 kgm^2
	Outer inertia	13,000 kgm^2
	Torsional stiffness	68 MNm/rad
	Damping	300 kN-m·s/rad
	Permissible elastic torque	703 kNm
	Permissible damping torque	101 kNm/bar
	Permissible thermal load	200 kW
	Required oil quantity	220 liter/min
Propeller	Type	FPP
	Moment of inertia in water	0.6385E+06 $kgm^2(mr^2)$
	Number of blades	6
	Diameter	9,100 mm
	Weight	105 ton

Table 2 Natural frequencies calculation[10]

Node	Calculated value (CPM)	Measured value(CPM)
1	164.92	About 165 (2.75 Hz)
2	628.71	About 660-670(11.0~11.2 Hz)
3	765.94	About 740 (12.3 Hz)

the intermediate shaft for the measurement of the torsional vibration stresses. The angular velocity was measured by Onosokki F-V converter 1300 and the gap sensor AEC PU-30 which was installed close to the turning wheel. Signal outputs were stored in a Sony 208A tape recorder while the FFT analyzer DI 2200 was used to analyze the acquired data.

3.1 12K98MC-Mk6 Engine with Chain Drive

As previously stated in this paper, torsional vibration stresses for the super large two stroke low speed diesel engine are said to exist and to be higher on the two node torsional vibration with a nodal point located in the crankshaft. The schematic diagram of mass system for 12K98MC engine is shown in Fig. 4.

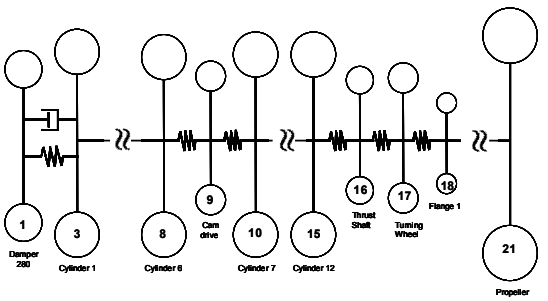

Fig. 4 Schematic diagram of mass system for 12K98MC engine

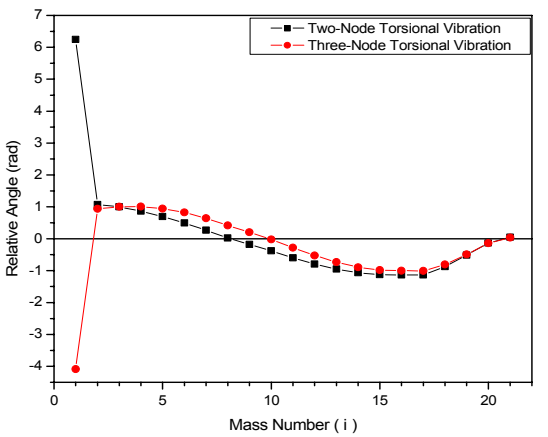

Fig. 5 Mode shapes of torsional vibrations for 12K98MC engine

Figure 5 represents the vibration mode of second and third node torsional vibration. It indicates the torsional stress of crankshaft for the 12K98MC engine, a nodal point at two node torsional vibrations is located between cylinder No. 6 and the chain drive for camshaft driving. The calculated natural frequency at the two node torsional vibration of the PSS is 73.61 rad/s before the damper was installed. Equivalent inertia moment and stiffness were also calculated as 317,428 kgm^2 and 173 MN-m/rad. The ratio of inertia moments (I_d / I) is about R=1/25.

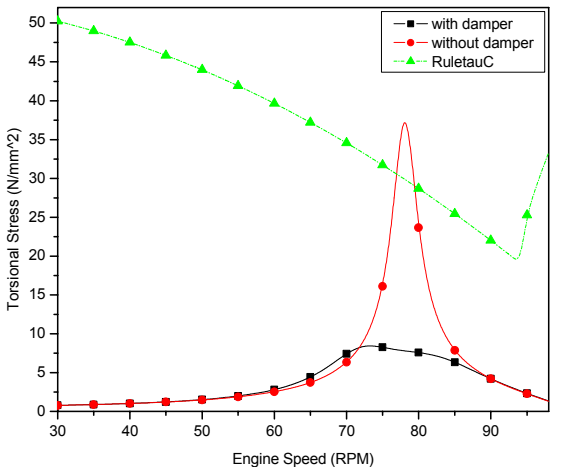

Fig. 6 Torsional vibration stress of crankshaft for the 12K98MC engine

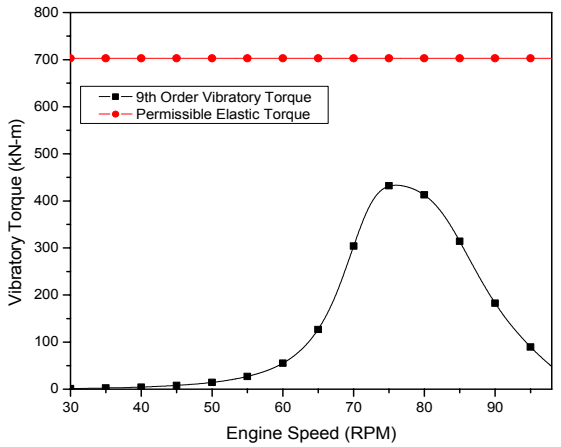

Fig. 7 Vibratory torque of D280/11 damper for 12K98MC engine

Figure 6 shows the calculation of torsional stresses of the PSS and the system's response with the damper installed. The calculated 9th order torsional stresses were 8.5 N/mm^2 at 73 RPM and 39 N/mm^2 at 78 RPM with damper and without damper respectively.

Figure 7 illustrates the Damper D280/11 design for permissible elastic torque which is 703 kN-m. The vibratory torque at the 9th order was measured to be around 430 kN-m.

Figures 8 and 9 compare the theoretical and measured angular velocities at the outer and inner damper. At Fig. 8, theoretical data indicated the damper's angular velocity peak value at 74 RPM to be 468 mrad/sec. However, actual measurements revealed higher angular velocities value at the outer damper nearing the engine's MCR. At 84 RPM, the calculated outer damper angular velocity indicates a reducing slope whereas the measured angular velocity had a little change in its value. A difference can be seen at the engine's MCR of 98 RPM wherein the calculated and measured angular velocity were established at around 125 and 280 mrad/sec and this condition within this

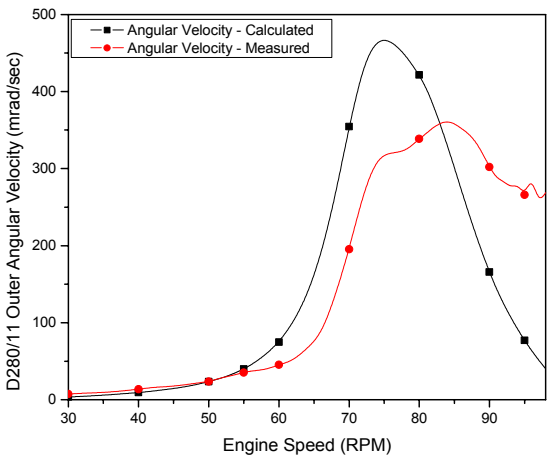

Fig. 8 The 9th order angular velocity of outer damper for 12K98MC engine

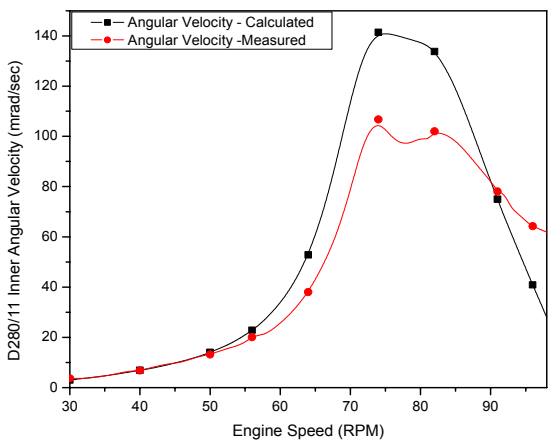

Fig. 9 The 9th order angular velocity of inner damper for 12K98MC engine

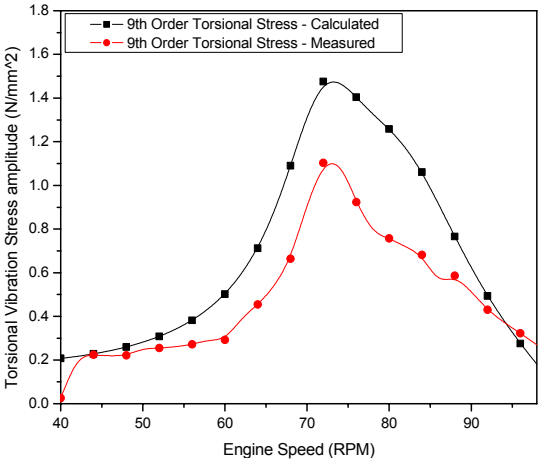

Fig. 10 The 9th order torsional vibration stress of intermediate shaft for 12K98MC engine

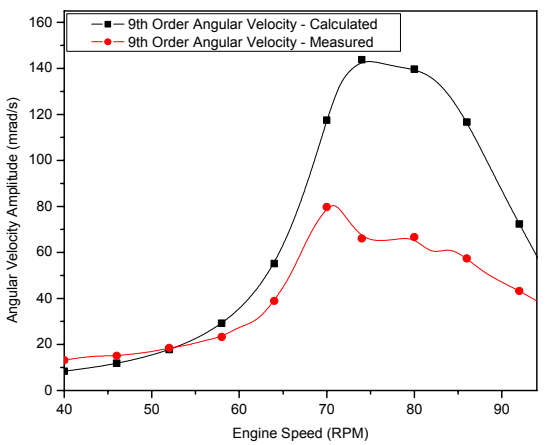

Fig. 11 The 9th order angular velocity of turning wheel for 12K98MC engine

range may be attributed to measurement errors at the Geislinger damper monitoring system.

For the inner angular velocity, Fig. 9 indicates the same pattern with that of the outer angular velocity. The measured and calculated values were confirmed at around 106 mrad/sec and 141 mrad/sec respectively at MCR.

The 9th order torsional vibration stress of the intermediate shaft is seen on Fig. 10. The calculated torsional stress is around 1.5 N/mm^2.

Measured values, however, indicated the torsional stress at 1.1 N/mm^2 at resonance peak 74 RPM.

Table 3 Specification for 12RT-flex96C-B Engine

Engine	Type	12RT-flex 96C-B
	Max. Continuous output	93,360.0 bhp
	Max. Continuous speed	102.0 rpm
	Cylinder bore	960.0 mm
	Stroke	2,500.0 mm
	Number of cylinder	12
	Mean indicated pressure	19.89 bar
	Ratio of connecting rod	0.434
	Reciprocating mass	17,834.0 kg/cyl
	Firing order	1-9-11-4-3-8-10-6-2-7-12-5
Damper	Type	Geislinger D260/28
	Inner inertia	540 kgm^2
	Outer inertia	9,760 kgm^2
	Torsional stiffness	57 MNm/rad
	Relative damping coefficient	240 kN-m·s/rad
	Permissible elastic torque	653 kNm
	Permissible thermal load	160 kW
	Oil flow	160 liter/min
Propeller	Type	FPP
	Moment of inertia in air	0.310E+06 kgm^2
	Moment of inertia in water	0.422E+06 kgm^2
	Number of blades	6
	Diameter	9,700 mm

Table 4 Natural frequencies calculation[11]

Node	Calculated value(CPM)	Measured value(CPM)
1	196.81(3.28 Hz)	About 196(3.27 Hz)
2	652.94(10.88 Hz)	About 684(11.4 Hz)
3	790.84(13.18 Hz)	About 780(13.0 Hz)

The 9th order angular velocity of the turning wheel was measured to be 82 mrad/s at a resonance peak of 74 RPM(Fig. 11) compared to the calculated value of 141 mrad/s.

3.2 12RT-flex 96C-B Engine with Gear Drive

A 12RT-flex 96C-B engine having a shaft power of around 93,360 SHP at 102 RPM was used as the second study model and emphasis was likewise focused on the two node torsional vibration of the PSS.

From Fig. 13, the two node torsional vibration calculation located one nodal point between engine cylinder number 7 and cylinder number 6. The natural frequency before the damper was installed is 74.73 rad/s. Equivalent inertia moment and

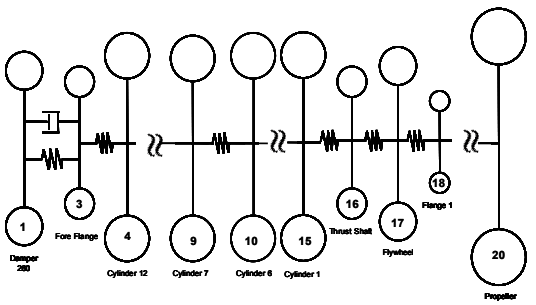

Fig. 12 Schematic diagram of mass system for 12RT-flex 96C-B engine

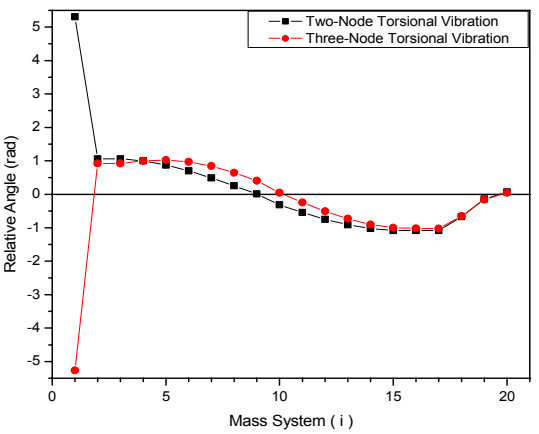

Fig. 13 Mode shapes of torsional vibrations for 12RT-flex 96C-B engine

stiffness were also calculated as 28,3708 kgm^2 and 159 MN-m/rad. The ratio of inertia moments (I_d / I) is about R=1/30.

Figure 14 shows the calculated torsional stresses to be 35 N/mm^2 at 78 RPM and 7.8 N/mm^2 at 73 RPM for without damper and with damper system respectively. In addition, it can be seen that for the undamped mass system, the torsional stress limit was barely exceeded. Hence, the use of a smaller damper size can be employed.

Figure 15 shows the vibratory torque at the 9th order to be around 357 kN-m at 76 RPM and the 653 kN-m permissible elastic torque limit.

Figures 16 and 17 shows the behaviour of the RT-flex engine's inner and outer damper. On Fig. 16, the outer damper peak resonance at 76 RPM has an angular velocity of 511 mrad/s for its calculated value while the actual measurements revealed the peak value to be around 400 mrad/s at 81 RPM. A noticeable deviation on the outer damper angular velocity nearing the MCR can be attributed again to measuring errors. Yet again, the measured data is evidently higher than the theoretical calculation.

For the inner damper, it exhibited a near identical value for the measured and calculated

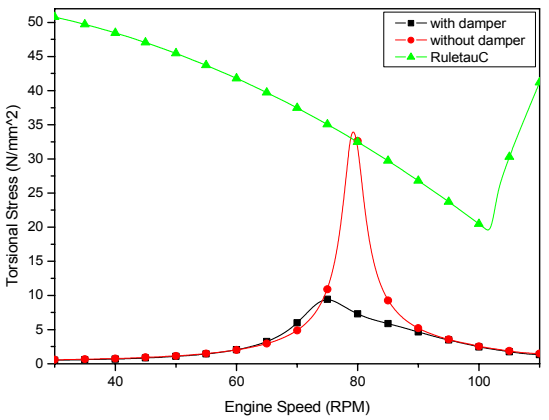

Fig. 14 The 9th order torsional vibration stress of crankshaft for the 12RT-flex 96C-B engine

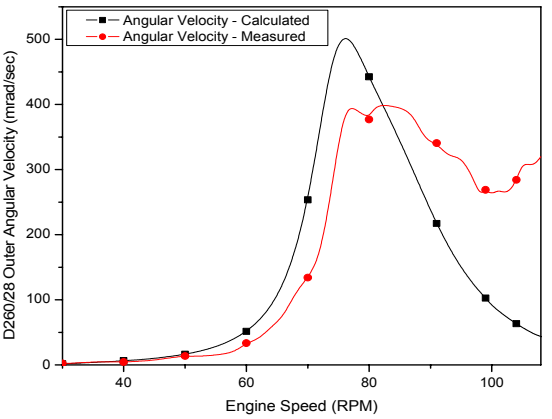

Fig. 16 The 9th order angular velocity of outer damper for 12RT-flex 96C-B engine

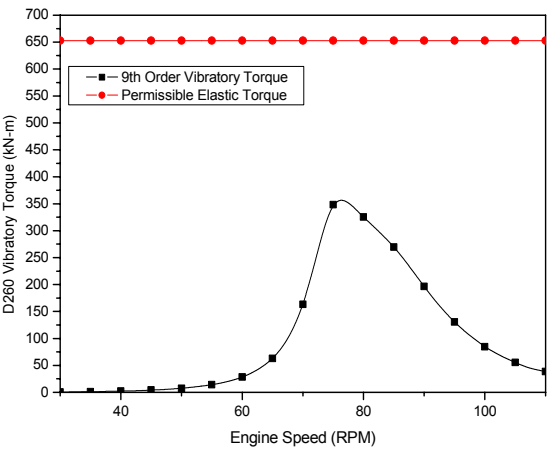

Fig. 15 The 9th order vibratory torque of D260/28 damper for 12RT-flex 96C-B engine

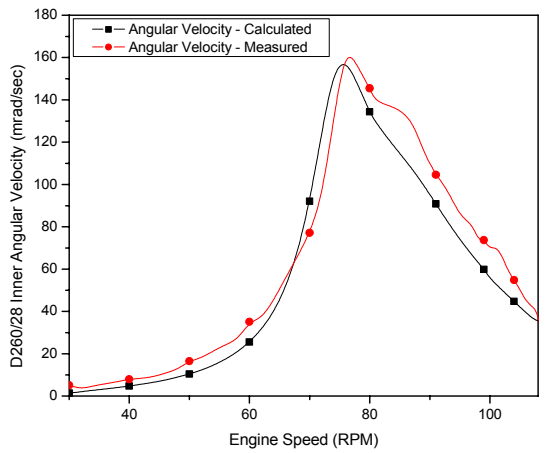

Fig. 17 The 9th order angular velocity of inner damper for 12RT-flex 96C-B engine

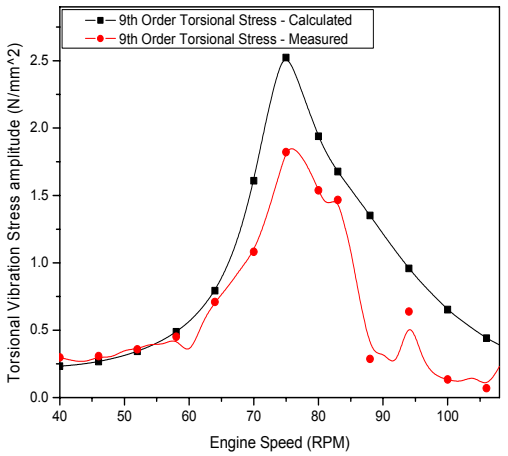

Fig. 18 The 9th order torsional vibration stress of intermediate shaft for 12RT-flex 96C-B

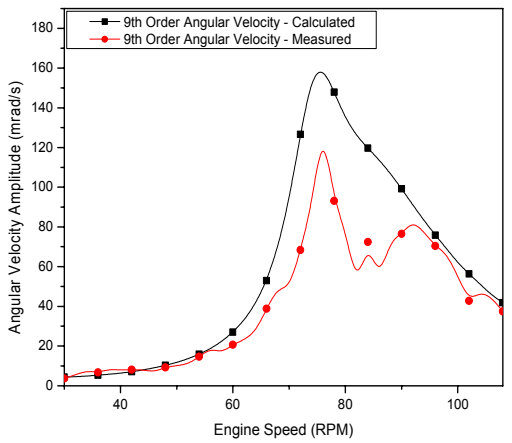

Fig. 19 The 9th order angular velocity of flywheel for 12RT-flex 96C-B

angular velocity(Fig. 17). The peak amplitude at 76 RPM shows a 159 mrad/s and 165 mrad/s angular velocity with the measured value a bit higher. Consequently, the calculated and measured angular velocity at MCR(102 RPM) is 50 mrad/s and 66 mrad/s

The 9th order torsional vibration stress of the intermediate shaft was measured to be 1.8 N/mm^2 at a resonance peak of 75 RPM(Fig. 18). Additionally, the 9th order angular velocity of the fly wheel was measured to be 135 mrad/s at a resonance peak of 74 RPM(Fig. 19) compared to the calculated value of 160 mrad/s.

4. Conclusion

For super large two stroke low speed diesel engines, the significant resonances and torsional stresses were exhibited at the 9th order of the two node torsional vibration with a nodal point located at the crankshaft of 12K98MC and 12RT-flex 96C-B. Hence, a tuning torsional vibration damper was designed and installed in these engines and investigated the dynamic characteristis of torsional vibration. The results are summarized as follows:

(1) For optimum tuning damper design, the multi-lumped mass system can be substituted with a two mass system for theoretical calculation. This method can be applied conveniently to tuning damper design.

(2) Four torsional vibration measuring points of the 12K98MC and 12RT-flex 96C-B engines were compared and evaluated. The calculated and measured torsional stresses of the crankshaft and intermediate shaft, and the outer damper angular velocity of both engines have shown proportional pattern. For 12K98MC engine with chaindrive and 12RT-flex 96C-B with gear drive, theoretical calculation of torsional vibration stresses at the crankshaft were reduced by 80 percent with the damper employed. In addition, measured torsional stresses and outer damper angular velocities is about 70 per cent of the theoretical calculations. Hence, the actual response of the PSS and the damping system can be predicted and referred for new designs.

(3) The vibration monitoring system of angular velocities at inner and outer has shown inaccuracies on the measurement values. Hence the data provided by the vibration monitoring system can check the damper function but will not provide precise data for the torsional vibration analysis of the propulsion shafting system.

(4) The dynamic response of 12RT-flex 96C-B engine's calculated and measured inner damper

angular velocities was found to be almost equal, though this can not be attributed solely on measurement errors, this circumstance necessitates further study.

References

(1) MAN B&W Diesel, 2006, First MAN B&W Diesel Engine Over 100000 BHP Now In Service, Press Release.

(2) Det Norske Veritas, Cost-saving Vibration Calculation for Shafting Systems, DNV.

(3) Lee, D. C., et al, 1992, "A Study on the Dynamic Characteristics and Performance of Geislinger Type Torsional Vibration Damper for Two stroke Low Speed Diesel Engines," Journal of the Korean Society of Marine Engineering, Vol 16, No. 5, pp. 329~340.

(4) MAN B&W, 1988, "Vibration Characteristics of Two Stroke Low Speed Diesel Engines," MAN B&W.

(5) MAN B&W, 2000, "An Introduction to Vibration Aspects of Two Stroke Diesel in Ships," MAN B&W.

(6) Hyundai Heavy Industries Co. Ltd., 1993, "Dynamic Characteristics and Performance of Tuning Torsional Vibration Damper for Hyundai – MAN B&W Two Stroke Low Speed Diesel Engine," MAN B&W Diesel AS, Meeting of Licensees.

(7) Nestorides, E. J., 1958, "A Handbook on Torsional Vibration, BICERA Research Laboratory," Cambridge University Press.

(8) Wachel, J. C., Szenazi F. R., 1993, "Analysis of Torsional Vibrations in Rotating Machinery," 22nd TurboMachinery Symposium.

(9) Rao, Singiresu S, 2004, "Mechanical Vibrations – Fourth Edition," Pearson – Prentice Hall.

(10) Dynamics Laboratory of MMU, 2006, "Torsional Vibration Measurement for Hyundai-Samho Container Ship," Document No. MDL- 06051.

(11) Dynamics Laboratory of MMU, 2006, "Torsional Vibration Measurement for Hyundai-Samho Container Ship," Document No. MDL-06101.